JOURNAL OF VIROLOGY, Aug. 2010, p. 8342–8347 Vol. 84, No. 16
0022-538X/10/$12.00 doi:10.1128/JVI.01470-09

Determinants in 3D^{pol} Modulate the Rate of Growth of Hepatitis A Virus$^{\nabla}$

Krishnamurthy Konduru and Gerardo G. Kaplan*

Laboratory of Hepatitis and Related Emerging Agents, DETTD-OBRR, Center for Biologics Evaluation and Research, Food and Drug Administration, Bethesda, Maryland 20892

Received 16 July 2009/Accepted 29 May 2010

Hepatitis A virus (HAV), an atypical member of the *Picornaviridae*, grows poorly in cell culture. To define determinants of HAV growth, we introduced a blasticidin (Bsd) resistance gene into the virus genome and selected variants that grew at high concentrations of Bsd. The mutants grew fast and had increased rates of RNA replication and translation but did not produce significantly higher virus yields. Nucleotide sequence analysis and reverse genetic studies revealed that a T6069G change resulting in a F42L amino acid substitution in the viral polymerase (3D^{pol}) was required for growth at high Bsd concentrations whereas a silent C7027T mutation enhanced the growth rate. Here, we identified a novel determinant(s) in 3D^{pol} that controls the kinetics of HAV growth.

Hepatitis A virus (HAV) is an atypical member of the *Picornaviridae* that replicates poorly in cell culture and generally does not cause cytopathic effect (CPE). The HAV positive-strand RNA genome of about 7.5 kb is encapsidated in a 27- to 32-nm icosahedral shell (12). The HAV genome contains a long open reading frame (ORF) that codes for a polyprotein of approximately 250 kDa, which undergoes co- and posttranslational processing by the virus-encoded protease 3C^{pro} into structural (VP0, VP3, and VP1-2A) and nonstructural proteins (11, 13, 14, 18). VP0 undergoes structural cleavage into VP2 and VP4, and an unknown cellular protease cleaves the VP1-2A precursor (9, 23).

HAV replicates inefficiently in cell culture and in general establishes persistent infections (3, 4, 7, 8) without causing CPE. However, some strains of HAV that replicate quickly can induce cell death (5, 19, 27). Due to the growth limitations, experimentation with HAV is difficult and the biology of this virus is poorly understood. To facilitate genetic studies, we recently introduced a blasticidin (Bsd) resistance gene at the 2A-2B junction of wild-type (wt) HAV (16). Bsd, an antibiotic that blocks translation in prokaryotes and eukaryotes and thus affects HAV translation, is inactivated by the Bsd-deaminase encoded in the Bsd resistance gene (15). Cells infected with the wt HAV construct carrying the Bsd resistance gene (HAV-Bsd) grew in the presence of Bsd. We have recently used the wt HAV-Bsd construct to select human hepatoma cell lines that support the stable growth of wt HAV (16) and to establish simple and rapid neutralization and virus titration assays (17). In this study, we developed a genetic approach to study determinants of HAV replication based on the selection of HAV-Bsd variants grown under increased concentrations of Bsd. We hypothesized that by increasing the concentration of Bsd, we would select HAV variants that grew better and allowed the survival of persistently infected cells at higher concentrations of the antibiotic. We also reasoned that we would need a robust HAV-Bsd replication system to provide enough Bsd-deaminase for cell survival. Therefore, we used attenuated HAV grown in rhesus monkey fetal kidney FRhK4 cells as an experimental system because (i) the virus grows 100-fold better in this system than wt HAV in human hepatoma cells (16), and (ii) it already contains cell culture-adapting mutations (3, 4, 7, 8) that are likely to accumulate during passage of wt HAV at high concentrations of Bsd and confound our analysis.

Attenuated HAV containing the Bsd gene allowed the survival of infected cells at low concentrations of Bsd. To test our hypothesis, we introduced a Bsd resistance gene into the genome of the attenuated HM-175 strain of HAV by overlap reverse transcription-PCR (RT-PCR) using the same strategy and primers described previously (16). Briefly, we first cloned a polylinker flanked by 3C^{pro} protease cleavage sites into the 2A-2B junction of the infectious cDNA of HAV in pT7HAV (29) to produce pHAVvec9 and then cloned the Bsd resistance gene into the polylinker to generate pHAVvec9-Bsd (Fig. 1A). All constructs were verified by automated nucleotide sequence analysis. To rescue viruses (16), linearized plasmids were transcribed *in vitro* with T7 RNA polymerase and transfected into FRhK4 cells. After 2 weeks of incubation at 35°C, cells were washed, lysed by three freeze-thaw cycles, and spun down. Supernatants containing the viral stocks were stored at −80°C. Viruses rescued from pT7HAV, pHAVvec9, and pHAVvec9-Bsd transfected cells were termed HAV/7, HAVvec9, and HAVvec9-Bsd, respectively. Immunofluorescence (IF) analysis staining with a neutralizing anti-HAV monoclonal antibody (MAb) revealed that FRhK4 cells infected with HAV/7, HAVvec9, and HAVvec9-Bsd had the characteristic cytoplasmic granular fluorescence of HAV-infected cells (Fig. 1B). The insertion of the polylinker had no effect in viral titers, but the Bsd resistance gene reduced 100-fold the HAV titers (Fig. 1C). As expected, FRhK4 cells infected with HAVvec9-Bsd but not with HAV/7, HAVvec9, or

* Corresponding author. Mailing address: Laboratory of Hepatitis and Related Emerging Agents, DETTD-OBRR, Center for Biologics Evaluation and Research, Food and Drug Administration, Bethesda, MD 20892. Phone: (301) 496-0338. Fax: (301) 480-7928. E-mail: gk@helix.nih.gov.

$^{\nabla}$ Published ahead of print on 9 June 2010.

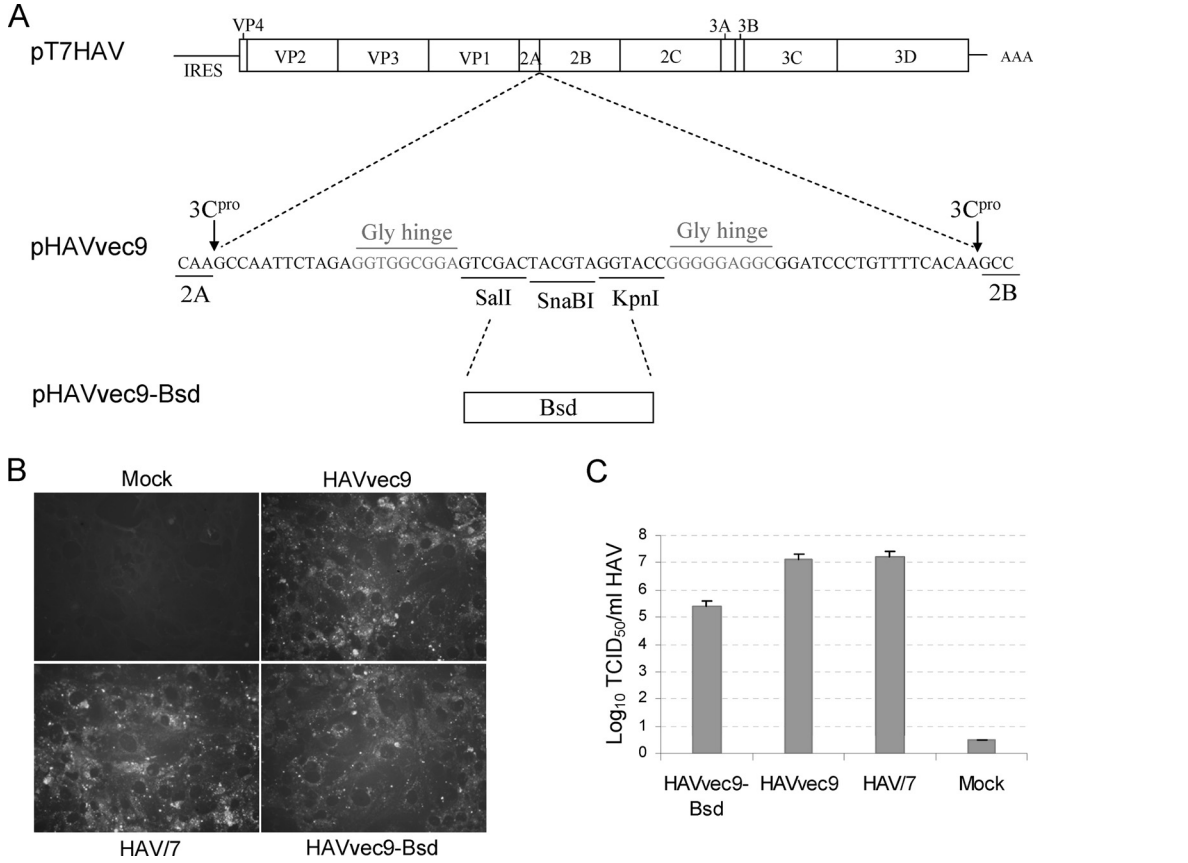

FIG. 1. Construction and rescue of cell culture-adapted HAV containing a Bsd selectable marker. (A) Schematic representation of HAV constructs. Synthetic oligonucleotides containing SalI, SnaBI, and KpnI restriction sites flanked by three G codons (Gly hinges) and HAV $3C^{pro}$ cleavage sites were cloned into the 2A-2B junction of the full-length infectious cDNA of cell culture-adapted strain HM-175 of HAV in pT7HAV (29). This construct, pHAVvec9, was cleaved with SalI and KpnI to insert a gene coding for Bsd-deaminase lacking translation initiation and termination codons (16) to generate pHAVvec9-Bsd. (B) Immunofluorescence (IF) analysis of HAV-infected cells. HAV/7, HAVvec9, and HAVvec9-Bsd were rescued from FRhK4 cells transfected with *in vitro*-synthesized HAV transcripts (16) from pT7HAV, pHAVvec9, and pHAVvec9-Bsd, respectively. FRhK4 cells were infected with virus stocks for 1 week, fixed, and stained with neutralizing anti-HAV MAb K2-4F2 as described previously (16). (C) Titration of HAV stocks. Tenfold serial dilutions of virus stocks were titrated in 96-well plates containing monolayers of African green monkey kidney cells. Plates were incubated for 2 weeks at 35°C, and viral titers were determined by an endpoint dilution enzyme-linked immunosorbent assay (ELISA) using rabbit anti-HAV antibodies as described previously (16). Viral titers and standard deviations, shown as bars, were calculated using the ID50 program developed by John L. Spouge (National Center for Biotechnology Information, NIH).

mock-infected cells survived selection with 1 μg/ml Bsd (Fig. 2A).

Selection of variants that grew at high concentrations of Bsd. To select viral variants capable of growing at higher levels of the antibiotic, we performed serial passages of HAVvec9-Bsd in FRhK4 cells at increasing concentrations of Bsd (Fig. 2B). Briefly, cells were infected with HAVvec9-Bsd at a multiplicity of infection (MOI) of 1 50% tissue culture infective dose ($TCID_{50}$)/cell and incubated for 6 weeks in the presence of Bsd. Cells were lysed, and viral stocks were prepared and used to infect naive FRhK4 cells at a higher concentration of Bsd. Serial passages under increasing concentrations of Bsd were performed at 1, 5, and 20 μg/ml Bsd but could not be continued at higher concentrations of the antibiotic because infected cells stopped growing at more than 20 μg/ml Bsd. Virus stocks produced at 1, 5, and 20 μg/ml Bsd, which were termed HAVvec9-Bsd, HAVvec9-Bsd-5, and HAVvec9-Bsd-20, respectively, had similar viral titers as assessed in FRhK4 cells (approximately 2×10^5 to 3×10^5 $TCID_{50}$/ml) and contained comparable genome equivalents (approximately 2×10^6 to 3×10^6 copies/ml) as determined by quantitative RT-PCR analysis (24). To analyze the variants grown at increased concentrations of Bsd, we infected FRhK4 cells with HAVvec9-Bsd, HAVvec9-Bsd-5, or HAVvec9-Bsd-20 for 1 week in the presence of 1, 5, or 20 μg/ml blasticidin and stained surviving cells with crystal violet (Fig. 2C). FRhK4-infected cells formed confluent monolayers at 1 μg/ml Bsd, whereas mock-infected cells did not survive the antibiotic selection. Only a few HAVvec9-Bsd-infected cells survived selection with 5 μg/ml Bsd (observed under the microscope), and none survived at 20 μg/ml Bsd. Cells infected with HAVvec9-Bsd-5 and -20 grew subconfluent monolayers at 5 μg/ml Bsd but only formed colonies at 20 μg/ml Bsd. A one-step growth curve analysis of the variants in FRhK4 cells using 2 μg/ml Bsd, a concentration of antibiotic that allowed the growth of all the tested viruses, showed that HAVvec9-Bsd-5 and -20 grew at similar rates but

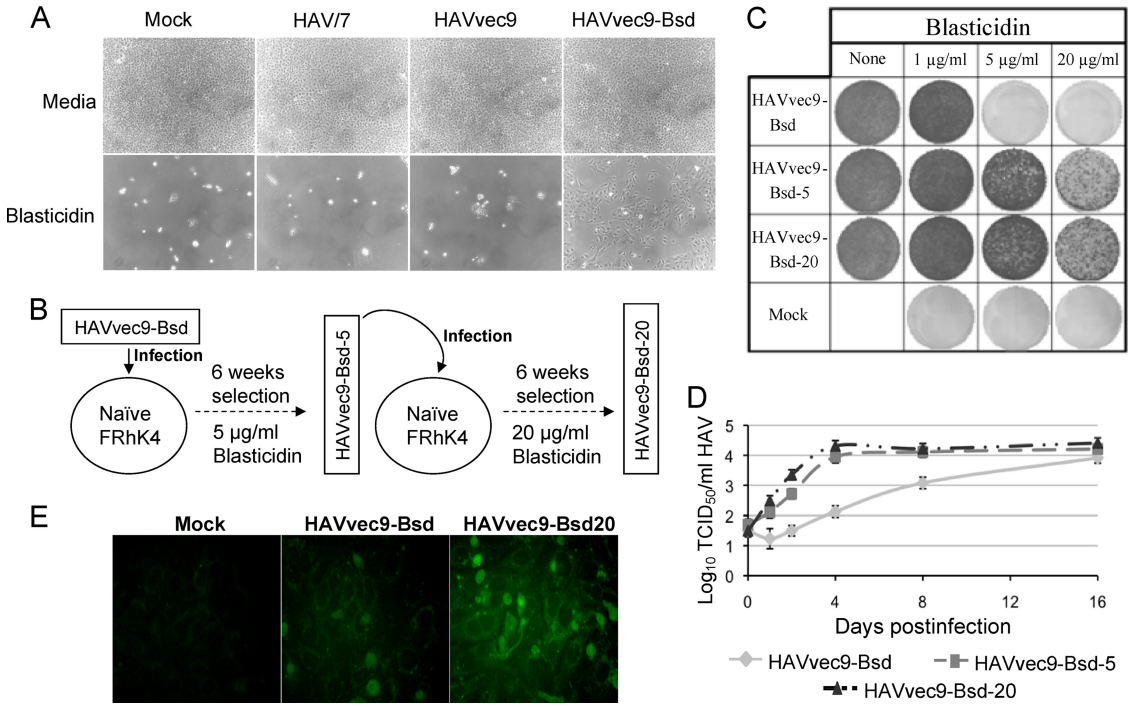

FIG. 2. Selection of HAVvec9-Bsd variants under increasing concentrations of Bsd. (A) FRhK4 cells infected with HAVvec9-Bsd survive selection with 1 μg/ml Bsd. Subconfluent monolayers of FRhK4 cells were infected with HAV/7, HAVvec9, or HAVvec9-Bsd at an MOI of 1 $TCID_{50}$/cell or mock infected and grown in a selection medium containing 1 μg/ml Bsd (16). Phase-contrast micrographs were taken in a Zeiss Axiscope microscope at ×200 magnification. (B) Schematic representation of the selection of HAVvec9-Bsd variants under increasing concentrations of Bsd. Serial passages of HAVvec9-Bsd in FRhK4 cells were performed under increasing concentrations of Bsd. To do so, FRhK4 cells were infected with HAVvec9-Bsd at an MOI of 1 $TCID_{50}$/cell and incubated for 6 weeks in the presence of Bsd. Viral stocks were prepared and used to infect naive FRhK4 cells at the following higher concentration of Bsd. Passages were performed at 1, 5, and 20 μg/ml Bsd, and the viral variants that grew at each concentration of the antibiotic were termed HAVvec9-Bsd, -5, and -20, respectively. (C) Growth of FRhK4 cells infected with *fr* HAV variants in the presence of different concentrations of Bsd. Subconfluent monolayers of FRhK4 cells in six-well plates were infected with HAVvec9-Bsd, -5, or -20 at an MOI of 1 $TCID_{50}$/cell or mock infected and selected with 1, 5, and 20 μg/ml Bsd. After 1 week of incubation at 35°C, cells were fixed with 5% trichloroacetic acid, stained with crystal violet, and photographed. Each image represents a well of the six-well plate. Cells that survived antibiotic selection and formed monolayers or grew in colonies were stained with the dye (dark areas). (D) One-step growth curve analysis of cells infected with HAVvec9-Bsd variants. FRhK4 cells were infected with an MOI of 2 to 5 $TCID_{50}$/cell of HAVvec9-Bsd, -5, or -20 in the presence of 2 μg/ml Bsd. At different times postinfection, virus stocks were prepared and titrated in 96-well plates containing FRhK4 cell monolayers in the presence of 2 μg/ml Bsd as described previously (17). Plates were observed under the microscope 8 days postinfection, and wells containing surviving cells were counted as positive. Viral titers and standard deviations, shown as error bars, were calculated using the ID50 program. (E) IF analysis of cells infected with HAV variants. IF analysis of FRhK4 cells mock infected or infected with HAVvec9-Bsd or HAVvec9-Bsd-20 for 4 days in the presence of 2 μg/ml Bsd was performed as described for Fig. 1B.

faster than HAVvec9-Bsd (Fig. 2D). However, these three variants reached similar viral yields at 16 days postinfection (dpi). To determine whether the difference in the growth rate was due to the asynchronous replication of the variants (2, 6, 10), we performed IF analysis staining with an anti-HAV MAb (Fig. 2E). At 4 dpi, a time point at which the variants reached the maximum titer differential, all cells in the monolayers contained viral antigens. Consequently, differences in asynchronous replication were not responsible for the increased growth rate of the variants. However, as judged by the intensity of the fluorescence signal, cells infected with HAVvev9-Bsd contained less HAV antigen than cells infected with HAVvev9-Bsd-20. Quantitative RT-PCR analysis (24) also showed that the kinetics of viral RNA replication was faster in HAVvec9-Bsd-20-infected cells than in HAVvec9-Bsd-infected cells (Fig. 3A). RNA replication of the HAV variants reached a maximum plateau at 3 dpi (data not shown), which contrasts with the burst at 3 dpi and further increase in RNA replication observed in slow-growing HAV strains (6). Western blot analysis of infected cells stained with rabbit anti-VP2 antibody (29), which reacts with viral capsid proteins VP2 and VP0, revealed higher levels of translation in HAVvec9-Bsd-20-infected cells than in HAVvec9-Bsd-infected cells (Fig. 3B, upper panel). Bands corresponding to a constitutive FRhK4 protein that cross-reacted with the rabbit anti-VP-2 antibody confirmed that similar amounts of total protein were loaded in each line (lower panel). Taken together, our data showed that the HAV variants selected under increased concentrations of Bsd grew faster than the parental virus. Therefore, we named these viruses fast-replicating (*fr*) HAV mutants.

Variants containing the coding T6069G and silent C7027T mutations in $3D^{pol}$ grew at high concentrations of Bsd. To study the HAV mutants in detail, we obtained six virus clones of each viral stock by endpoint dilution in 96-well plates containing FRhK4 cells. We then amplified the RNA of the viral clones by RT-PCR and performed automatic nucleotide se-

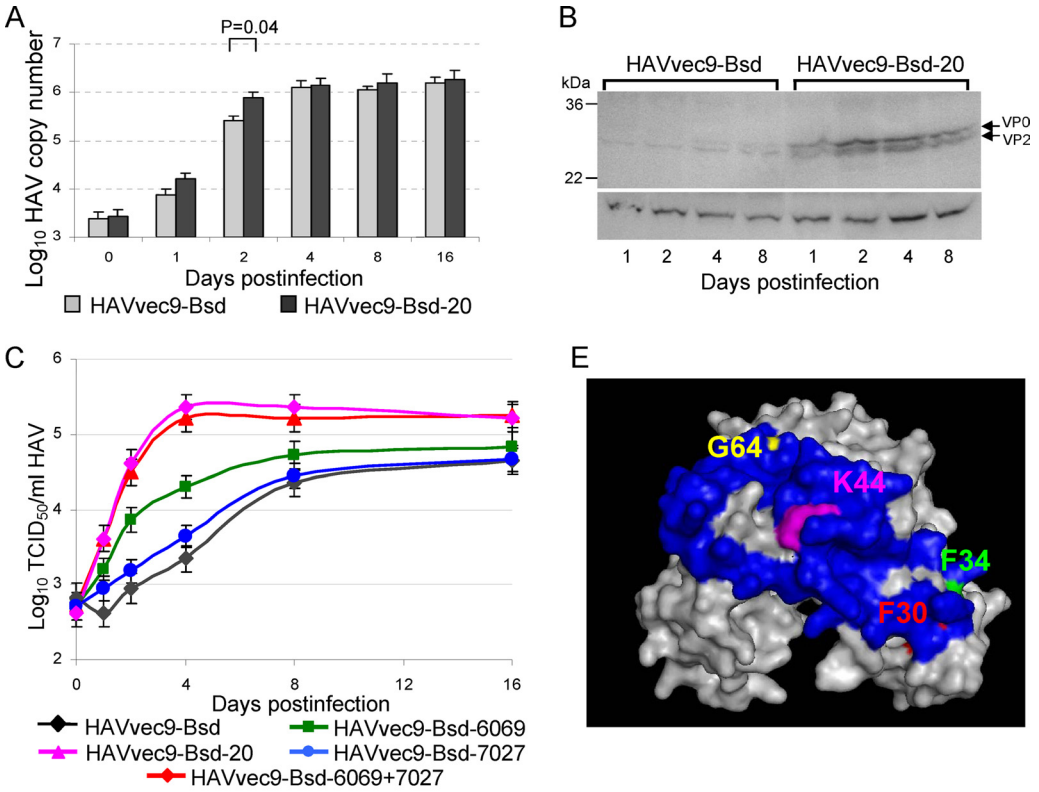

D

```
CV    GEIEFIESSKDAGFPVINTPSKTKLEPSVFHQVFEGNKE--PAVLRSGDPRLK-AN--FEEAIFSKYIGNVNTH--
PV    GEIQWMRPSKEVGYPIINAPSKTKLEPSAFHYVFEGVKE--PAVLTKNDPRLK-TD--FEEAIFSKYVGNKITE--
HRV   GQIQISKHVKDVGLPSIHTPTKTKLQPSVFYDIFPGSKE--PAVLTEKDPRLK-VD--FDSALFSKYKGNTECS--
FMDV  GLIVDTRDVEER----VHVMRKTKLAPTVAHGVFNPEFG--PAALSNKDPRLN-EGVVLDEVIFSKHKGDTKMTEE
HAV   -RIMKVEFTQCS----MNVVSKTLFRKSPIYHHIDKTMINFPAAMPFSKAEIDPMAVMLSKYSLPIVEEPEDYK--
```

FIG. 3. Characterization of HAVvec9-Bsd variants. (A) Analysis of HAV RNA replication by quantitative RT-PCR. Total RNA was extracted from FRhK4 cells infected with an MOI of 2 to 5 $TCID_{50}$/cell of HAVvec9-Bsd or -20 at different times postinfection. HAV RNA was quantitated by real-time RT-PCR as described previously (24). The HAV RNA copy numbers were determined in triplicate and expressed as mean values with standard deviations shown as error bars. Statistical significance at 2 days postinfection was determined by *t* test. (B) Western blot analysis of HAV-infected cells. FRhK4 cells were infected with an MOI of 2 to 5 $TCID_{50}$/cell of HAVvec9-Bsd or -20, cell extracts were prepared at different dpi, and equal amounts of extracts were resolved by 4 to 12% SDS-PAGE under denaturing conditions, transferred to polyvinylidene difluoride (PVDF) membranes, and probed with rabbit anti-HAV VP2 antibodies as described previously (29). Bands corresponding to VP0 and VP2 specifically detected by the anti-VP2 antibodies are marked with arrows (upper panel). Bands corresponding to a constitutive FRhK4 cellular protein that cross-reacted with the anti-VP2 antibodies are shown as loading controls (lower panel). Molecular size markers are indicated in kilodaltons. (C) Mutations in $3D^{pol}$ that increased the growth kinetics of the HAVvec9-Bsd variants. The T6069G, mutation, the C7027T mutation, or both mutations were introduced into the infectious cDNA of HAVvec9-Bsd to generate HAVvec9-Bsd-6069, HAVvec9-Bsd-7027, and HAVvec9-Bsd-6069 + 7027, respectively. One-step growth curve analysis of constructs and variants in FRhK4 cells was done as described for Fig. 2D. (D) Alignment of $3D^{pol}$ N-terminal 69-amino-acid sequences of HAV and other members of the *Picornaviridae*. Single-letter amino acid symbols of $3D^{pol}$ from coxsackievirus (CV) B3, poliovirus (PV), human rhinovirus (HRV), foot-and-mouth virus (FMDV), and hepatitis A virus (HAV), corresponding to accession numbers AAW83322, NP_740478, 1XR7B, CAA59731, and AAA45466, respectively, were aligned using the Clustal W program, which introduced gaps in the sequence shown as dashes. Conserved KT and PAA/V motifs are shown in blue, and the HAV F42, which changed to L due to the T6069G mutation, is shown in magenta. (E) Space-filling model of the poliovirus $3D^{pol}$ (1RA6) (26) showing amino acids F30 (red), F34 (green), K44 (magenta), and G64 (yellow) and the remaining N-terminal 69 amino acids that from the "index finger" in blue.

quence analysis of the complete HAV genomes (Table 1). All the HAVvec9-Bsd clones had the same sequence, which was identical to that of the input virus. Therefore, insertion of the Bsd gene, with no further selection, permitted the survival of cells at 1 μg/ml Bsd with no changes in viral RNA sequence. The survival of a few HAVvec9-Bsd-infected cells at 5 μg/ml Bsd suggested the presence of a small proportion of mutants capable of supporting cell growth at higher levels of the antibiotic. All the HAVvec9-Bsd-5 clones contained a silent C7027T change in $3D^{pol}$. Four of the HAVvec9-Bsd-5 clones contained a T6069G mutation in addition to the C7027T change and grew well at 1, 5, and 20 μg/ml Bsd. It should be pointed out that the T6069G mutation resulted in an F-to-L amino acid change at amino acid 42 of $3D^{pol}$ (F42L). Interestingly, the two HAVvec9-Bsd-5 clones that only had the silent C7027T change did not grow at 20 μg/ml Bsd. Five HAVvec9-Bsd-20 clones that contained the C7027T and T6069G changes plus two additional silent mutations, C5545T and C6780T, grew well at all the tested concentrations of Bsd. The remaining HAVvec9-Bsd-20 clone, which did not grow in 20 μg/ml

TABLE 1. Nucleotide sequence analysis of HAV clones and constructs grown at different concentrations of blasticidin

Virus[a]	Mutation position in the HAV genome[b]								Cell growth in blasticidin (μg/ml)[c]		
	5545 (nt)	$3C^{pro}$ (aa)	6069 (nt)	$3D^{pol}$ (aa)	6780 (nt)	$3D^{pol}$ (aa)	7027 (nt)	$3D^{pol}$ (aa)	1	5	20
HAV/7	C	L	T	F	C	I	C	L	−	−	−
HAVvec9-Bsd[d]	C	L	T	F	C	I	C	L	+	+/−	−
HAVvec9-Bsd-5											
4 clones	C	L	**G**	**L**	C	I	**T**	L	+	+	+
2 clones	C	L	T	F	C	I	**T**	L	+	+/−	−
HAVvec9-Bsd-20											
5 clones	**T**	L	**G**	**L**	**T**	I	**T**	L	+	+	+
1 clone	**T**	L	T	F	**T**	I	**T**	L	+	+/−	−
HAVvec9-Bsd-6069	C	L	**G**	**L**	C	I	C	L	+	+	+
HAVvec9-Bsd-7027	C	L	T	F	C	I	**T**	L	+	+/−	−
HAVvec9-Bsd-6069 + 7027	C	L	**G**	**L**	C	I	**T**	L	+	+	+

[a] The HAV/7 nucleotide sequence was obtained from the infectious HAV cDNA in pT7HAV. The sequences of six clones of HAVvec9-Bsd, -5, and -20 were obtained by RT-PCR and automatic sequencing of the whole viral genome. HAVvec9-Bsd-6069, HAVvec9-Bsd-7027, and HAVvec9-Bsd-6069 + 7027 were rescued from FRhK4 cells transfected with T7 polymerase *in vitro* transcripts from pHAVvec9-Bsd constructs containing T6069G, C7027T, and both T6069G and C7027T mutations, respectively. The nucleotide sequence of the rescued viruses was obtained by RT-PCR and automatic sequencing. Mutations were identified at nucleotides only at positions 5545, 6069, 6780, and 7027.

[b] HAV genome nucleotide (nt) sequence at positions 5545 in the protease ($3C^{pro}$) and 6069, 6780, and 7027 in the polymerase ($3D^{pol}$). Corresponding amino acid (aa) residues at the codons defined by the nucleotide positions. Changes in nucleotide and amino acid positions are indicated by bold characters.

[c] After infection, cells were selected with 1 or 5 or 20 μg/ml blasticidin, and presence (+) of blasticidin-resistant colonies, absence (-) of surviving cells, or presence of few surviving cells that did not form colonies (+/−) was determined at 7 dpi under the microscope.

[d] Six clones were sequenced, and all contained the same nucleotides at positions 5545, 6069, 6780, and 7027.

Bsd, contained the same three silent mutations but lacked the T6069G change. These data suggested that the coding T6069G mutation but not the silent C5545T and C6780T mutations was required for the *fr* phenotype and resistance to 20 μg/ml Bsd. However, the role of the C7027T mutation in the *fr* phenotype remained elusive.

The coding T6069G mutation is necessary and sufficient for growth at high concentrations of Bsd. To further determine the role of the T6069G in the *fr* phenotype, we engineered the mutation into the infectious HAVvec9-Bsd cDNA using overlap PCR and synthetic oligonucleotides containing single-nucleotide substitutions as described previously (16). The virus was rescued in FRhK4 cells, and the presence of the introduce mutation was verified by RT-PCR and nucleotide sequence analysis. The HAVvec9-Bsd mutant containing the coding T6069G change, termed HAVvec9Bsd-6069, grew faster than HAVvec9-Bsd but slower than HAVvec9-Bsd-20 in FRhK4 cells (Fig. 3C), indicating that the T6069G mutation partially restored the *fr* phenotype. Interestingly, HAVvec9Bsd-6069 grew at 20 μg/ml Bsd (Table 1), indicating that the increase in the replication rate allowed the survival of infected cells at higher concentrations of the antibiotic.

The silent C7027T mutation enhanced but was not sufficient to confer the *fr* phenotype. Similarly, we introduced the C7027T change into the infectious cDNA of HAVvec9-Bsd and analyzed the phenotype of the rescued virus. The mutant containing the C7027T change, termed HAVvec9Bsd-7027, grew slowly and at the same rate than parental HAVvec9-Bsd (Fig. 3C), indicating that the C7027T mutation alone did not confer the *fr* phenotype. Moreover, HAVvec9Bsd-7027 did not grow at 20 μg/ml Bsd (Table 1). The mutant containing both the T6069G and C7027T, termed HAVvec9-Bsd-6069 + 7027, grew as fast as HAVvec9-Bsd-20, indicating that the silent C7027T change had a synergistic effect and enhanced the replication rate conferred by the T6069G coding mutation. As expected, HAVvec9-Bsd-6069 + 7027 grew at 20 μg/ml Bsd (Table 1). Therefore, these two mutations were required to convey the full *fr* phenotype observed in HAVvec9-Bsd-20.

The F42 residue maps to the middle of the "index finger" of $3D^{pol}$. It was of interest to map the location of the F42 residue in $3D^{pol}$ affected by the mutation in nucleotide 6069. Alignment of the first 69 amino acid residues of $3D^{pol}$ of HAV with other members of the *Picornaviridae* (Fig. 3D) revealed that two amino acid motifs, KT and PAV/A (shown in blue), are highly conserved in the family. The HAV F42 (magenta) is 3 residues from the PAV/A motif and aligned with K44 of the PV $3D^{pol}$, for which the crystal structure has been resolved at high resolution (26). Although the HAV $3D^{pol}$ has not been crystallized, $3D^{pol}$ structures are conserved in the *Picornaviridae* (20), so the HAV F42 is likely to be in the proximity of the PV K44. According to the analogy of the "right hand" shape with the structure of $3D^{pol}$ (Fig. 3E), the N-terminal 69 amino acid residues of PV $3D^{pol}$ form an "index finger" (residues in blue) (26) with PV K44 (magenta) lying in the middle. The fingers of $3D^{pol}$ are very flexible and exist in a highly dynamic molten globule state at physiological temperature (25). The "index finger" plays an important role in maintaining this flexibility and the function of $3D^{pol}$ (25). Residues at the tip of the "index finger" such as F30 (red) and F34 (green) in the PV $3D^{pol}$ interact with the top of the "thumb" and are important for the proper function of the polymerase (25). The G64 residue at the top of the "index finger" in PV $3D^{pol}$ (yellow) modulates the catalytic site of $3D^{pol}$ (1, 21, 26), and the G64S change reduced the rate for nucleotide incorporation of the enzyme (20, 26). Our results suggested that the HAV F42L change had the opposite effect and increased the kinetics of

RNA replication (Fig. 3A) and HAV growth (Fig. 3C). In humans, wt HAV has a long incubation period of 7 to 50 days that could be attributed to the slow replication rate limiting the spread of the virus. In cell culture, wt HAV also grows slowly without causing CPE (16). Therefore, it is likely that HAV contains determinants capable of limiting its replication, such as the ones we identified in T6069 and C7027, to prevent cell damage and escape immune surveillance.

In this study, we showed that a T6069G mutation that resulted in the F42L amino acid change in $3D^{pol}$ increased the rate of RNA replication and HAV-specific translation. Interestingly, the faster kinetics of HAV growth did not result in an increased virus yield, indicating that other limiting factors in the life cycle of HAV, such as the use of rare codons (22) or the availability of cellular factors, are also responsible for its poor growth. The silent C7027T mutation in the $3D^{pol}$ that synergized with the T6069G change but was not sufficient to increase the rate of growth of the virus (Fig. 3C) suggested that RNA structure and/or codon utilization also played a role in the *fr* phenotype. Recently, a *cis*-acting replication element (*cre*) was identified between nucleotides 5948 and 6057 of the HAV genome in the $3D^{pol}$ gene (28). Since nucleotide 6069 is adjacent to the *cre* element, we cannot rule out the possibility that the T6069G change affected the structure of the *cre*, increasing the rate of RNA replication. Our attempts to rescue viruses containing a silent mutation at nucleotide 6069 have been unsuccessful. Further research will be required to determine whether the *fr* phenotype was due to the F42L change in $3D^{pol}$, the effect of the T6069G change in the *cre*, or both. The $3D^{pol}$ mutants described herein could be used to shorten the time required to produce HAV antigen and reduce the cost of vaccine production.

This work was supported by intramural research funds from the Food and Drug Administration (FDA) to G.G.K.

The findings and conclusions in this article have not been formally disseminated by the FDA and should not be construed to represent any FDA determination or policy.

We thank Susan Zullo and Jérôme Jacques for critical reviews of the manuscript.

REFERENCES

1. **Arnold, J. J., M. Vignuzzi, J. K. Stone, R. Andino, and C. E. Cameron.** 2005. Remote site control of an active site fidelity checkpoint in a viral RNA-dependent RNA polymerase. J. Biol. Chem. **280:**25706–25716.
2. **Cho, M. W., and E. Ehrenfeld.** 1991. Rapid completion of the replication cycle of hepatitis A virus subsequent to reversal of guanidine inhibition. Virology **180:**770–780.
3. **Cohen, J. I., B. Rosenblum, S. M. Feinstone, J. Ticehurst, and R. H. Purcell.** 1989. Attenuation and cell culture adaptation of hepatitis A virus (HAV): a genetic analysis with HAV cDNA. J. Virol. **63:**5364–5370.
4. **Cohen, J. I., J. R. Ticehurst, R. H. Purcell, A. Buckler-White, and B. M. Baroudy.** 1987. Complete nucleotide sequence of wild-type hepatitis A virus: comparison with different strains of hepatitis A virus and other picornaviruses. J. Virol. **61:**50–59.
5. **Cromeans, T., M. D. Sobsey, and H. A. Fields.** 1987. Development of a plaque assay for a cytopathic, rapidly replicating isolate of hepatitis A virus. J. Med. Virol. **22:**45–56.
6. **de Paula, V. S., A. S. Perse, L. A. Amado, L. M. de Morais, S. M. de Lima, R. S. Tourinho, A. M. Gaspar, and M. A. Pinto.** 2009. Kinetics of hepatitis A virus replication in vivo and in vitro using negative-strand quantitative PCR. Eur. J. Clin. Microbiol. Infect. Dis. **28:**1167–1176.
7. **Emerson, S. U., C. McRill, B. Rosenblum, S. Feinstone, and R. H. Purcell.** 1991. Mutations responsible for adaptation of hepatitis A virus to efficient growth in cell culture. J. Virol. **65:**4882–4886.
8. **Frosner, G. G., F. Deinhardt, R. Scheid, V. Gauss-Muller, N. Holmes, V. Messelberger, G. Siegl, and J. J. Alexander.** 1979. Propagation of human hepatitis A virus in a hepatoma cell line. Infection **7:**303–305.
9. **Graff, J., O. C. Richards, K. M. Swiderek, M. T. Davis, F. Rusnak, S. A. Harmon, X. Y. Jia, D. F. Summers, and E. Ehrenfeld.** 1999. Hepatitis A virus capsid protein VP1 has a heterogeneous C terminus. J. Virol. **73:**6015–6023.
10. **Harmon, S. A., D. F. Summers, and E. Ehrenfeld.** 1989. Detection of hepatitis A virus RNA and capsid antigen in individual cells. Virus Res. **12:**361–369.
11. **Harmon, S. A., W. Updike, X. Y. Jia, D. F. Summers, and E. Ehrenfeld.** 1992. Polyprotein processing in cis and in trans by hepatitis A virus 3C protease cloned and expressed in *Escherichia coli*. J. Virol. **66:**5242–5247.
12. **Hollinger, F. B., and S. U. Emerson.** 2008. Hepatitis A virus, p. 911–948. *In* D. M. Knipe and P. M. Howley (ed.), Fields virology, 4th ed., vol. 1. Lippincott Williams & Wilkins, Philadelphia, PA.
13. **Jansen, R. W., J. E. Newbold, and S. M. Lemon.** 1988. Complete nucleotide sequence of a cell culture-adapted variant of hepatitis A virus: comparison with wild-type virus with restricted capacity for in vitro replication. Virology **163:**299–307.
14. **Jia, X. Y., D. F. Summers, and E. Ehrenfeld.** 1993. Primary cleavage of the HAV capsid protein precursor in the middle of the proposed 2A coding region. Virology **193:**515–519.
15. **Kimura, M., A. Takatsuki, and I. Yamaguchi.** 1994. Blasticidin S deaminase gene from Aspergillus terreus (BSD): a new drug resistance gene for transfection of mammalian cells. Biochim. Biophys. Acta **1219:**653–659.
16. **Konduru, K., and G. G. Kaplan.** 2006. Stable growth of wild-type hepatitis A virus in cell culture. J. Virol. **80:**1352–1360.
17. **Konduru, K., M. L. Virata-Theimer, M. Y. Yu, and G. G. Kaplan.** 2008. A simple and rapid hepatitis A virus (HAV) titration assay based on antibiotic resistance of infected cells: evaluation of the HAV neutralization potency of human immune globulin preparations. Virol. J. **5:**155.
18. **Martin, A., N. Escriou, S. F. Chao, M. Girard, S. M. Lemon, and C. Wychowski.** 1995. Identification and site-directed mutagenesis of the primary (2A/2B) cleavage site of the hepatitis A virus polyprotein: functional impact on the infectivity of HAV RNA transcripts. Virology **213:**213–222.
19. **Nasser, A. M., and T. G. Metcalf.** 1987. Production of cytopathology in FRhK-4 cells by BS-C-1-passaged hepatitis A virus. Appl. Environ. Microbiol. **53:**2967–2971.
20. **Ng, K. K., J. J. Arnold, and C. E. Cameron.** 2008. Structure-function relationships among RNA-dependent RNA polymerases. Curr. Top. Microbiol. Immunol. **320:**137–156.
21. **Pfeiffer, J. K., and K. Kirkegaard.** 2003. A single mutation in poliovirus RNA-dependent RNA polymerase confers resistance to mutagenic nucleotide analogs via increased fidelity. Proc. Natl. Acad. Sci. U. S. A. **100:**7289–7294.
22. **Pinto, R. M., L. Aragones, M. I. Costafreda, E. Ribes, and A. Bosch.** 2007. Codon usage and replicative strategies of hepatitis A virus. Virus Res. **127:**158–163.
23. **Rachow, A., V. Gauss-Muller, and C. Probst.** 2003. Homogeneous hepatitis A virus particles. Proteolytic release of the assembly signal 2A from procapsids by factor Xa. J. Biol. Chem. **278:**29744–29751.
24. **Silberstein, E., L. Xing, W. van de Beek, J. Lu, H. Cheng, and G. G. Kaplan.** 2003. Alteration of hepatitis A virus (HAV) particles by a soluble form of HAV cellular receptor 1 containing the immunoglobin-and mucin-like regions. J. Virol. **77:**8765–8774.
25. **Thompson, A. A., R. A. Albertini, and O. B. Peersen.** 2007. Stabilization of poliovirus polymerase by NTP binding and fingers-thumb interactions. J. Mol. Biol. **366:**1459–1474.
26. **Thompson, A. A., and O. B. Peersen.** 2004. Structural basis for proteolysis-dependent activation of the poliovirus RNA-dependent RNA polymerase. EMBO J. **23:**3462–3471.
27. **Venuti, A., C. Di Russo, N. del Grosso, A. M. Patti, F. Ruggeri, P. R. De Stasio, M. G. Martiniello, P. Pagnotti, A. M. Degener, M. Midulla, et al.** 1985. Isolation and molecular cloning of a fast-growing strain of human hepatitis A virus from its double-stranded replicative form. J. Virol. **56:**579–588.
28. **Yang, Y., M. Yi, D. J. Evans, P. Simmonds, and S. M. Lemon.** 2008. Identification of a conserved RNA replication element (*cre*) within the $3D^{pol}$-coding sequence of hepatoviruses. J. Virol. **82:**10118–10128.
29. **Zhang, Y., and G. G. Kaplan.** 1998. Characterization of replication-competent hepatitis A virus constructs containing insertions at the N terminus of the polyprotein. J. Virol. **72:**349–357.